Available online at www.sciencedirect.com
ScienceDirect
Journal of Fluorine Chemistry 128 (2007) 1227–1234
JOURNAL OF FLUORINE CHEMISTRY
www.elsevier.com/locate/fluor

Reactivity of fluorinated sulfur-containing heterocycles towards nucleophilic and oxidizing reagents

Viacheslav A. Petrov [a,*], Steve Lustig [a], Will Marshall [b]

[a] DuPont Central Research and Development, Experimental Station, P.O. Box 80328, Wilmington, DE 19880-0328, USA[1]

[b] DuPont Corporate Center for Analytical Sciences, Experimental Station, P.O. Box 80328, Wilmington, DE 19880-0328, USA

Received 24 March 2007; received in revised form 11 May 2007; accepted 12 May 2007
Available online 17 May 2007

Abstract

The reaction of 5,5-bis(trifluoromethyl)-6-thia-bicyclo[2.2.1]hept-2-ene, 5,5-bis(trifluoromethyl)-6-thia-bicyclo[2.2.2]oct-2-ene and 2,2-bis(trifluoromethyl)-3,6-dihydro-4,5-dimethyl-2*H*-thiopyran with *i*-C_3H_7MgCl leads to the formation of ring opening products as the result of nucleophilic attack of the Grignard reagent on the sulfur atom. According to DFT calculations the reactivity of the sulphur-containing substrate correlates with the strain energy of the heterocycle. The oxidation of 3-thia-4,4-bis(trifluoromethyl) tricyclo[5.2.1.$0^{2,5}$]non-7-ene by hydrogen peroxide in hexafluoro-*iso*-propanol solvent resulted in formation of the corresponding sulfoxide however, the reaction with *m*-chloroperoxybenzoic acid produced the product of exhaustive oxidation of sulfur and the double bond. In sharp contrast, the oxidation of 5,5-bis(trifluoromethyl)-6-thia-bicyclo[2.2.1]hept-2-ene and 5,5-bis(trifluoromethyl)-6-thia-bicyclo[2.2.2]oct-2-ene by MCPBA (2d, 25 °C) proceeds with the preservation of the double bond, leading to the selective formation of the corresponding sulfones.

Keywords: Diels–Alder adducts of hexafluorothioacetone; Reaction with *iso*-propyl magnesium chloride; Oxidation; *m*-Chloroperoxybenzoic acid

1. Introduction

A variety of cyclic polyfluorinated sulfides are readily available through the reaction of cyclic dimer of hexafluorothioacetone (HTFA) – 2,2,4,4-tetrakis-(trifluoromethyl)-1,3-dithietane – with hydrocarbon dienes, polyenes and activated olefins [1–5]. Surprisingly, the chemistry of the cycloadducts is limited to a few chemical transformations reported for 4-alkoxy-2,2-bis(trifluoromethyl)thietanes (cycloadducts of HFTA with vinyl ethers) [3] and 3-thia-4,4-bis(trifluoromethyl)tricyclo[5.2.1.$0^{2,5}$]non-7-ene (**1**, cycloadduct of HFTA and quadricyclane) [6]. Since the reactivity of both groups of materials towards nucleophilic reagents is defined by the positive charge on the sulfur of the heterocycle, it was reasonable to believe that other cycloadducts of HFTA will have similar reactivity. On the other hand, the ability of sulfides to undergo oxidation offered an opportunity for the synthesis of new polyfluorinated sulfoxides and sulfones.

This paper summarizes new data on reactions of HFTA cycloadducts with *i*-C_3H_7MgCl and oxidizing agents.

2. Results and discussion

2.1. Reaction with *i*-C_3H_7MgCl

Recently, we have demonstrated that 3-thia-4,4-bis(trifluoromethyl)tricyclo[5.2.1.$0^{2,5}$]non-7-ene (**1**) [5] rapidly reacts with organo-lithium or magnesium reagents under mild conditions [6]. Ring opening process results in selective formation of the corresponding norbornenes with an *exo*-orientation of both substituents. For example, the reaction of **1** and *i*-C_3H_7MgCl (**2**) rapidly proceeds in

* Corresponding author. Tel.: +1 3026951958; fax: +1 3026958281.
E-mail address: viacheslav.a.petrov@usa.dupont.com (V.A. Petrov).

[1] Publication no. 8781.

0022-1139/$ – see front matter © 2007 Elsevier B.V. All rights reserved.
doi:10.1016/j.jfluchem.2007.05.009

THF at 0–5 °C producing compound **3** in 84% yield [6] (Eq. (1)):

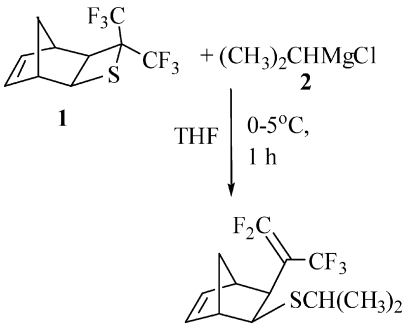

(1)

3, 84%

Surprisingly, containing a less strained six-membered heterocyclic ring 5,5-bis(trifluoromethyl)-6-thia-bicyclo[2.2.1]-hept-2-ene (**4**) was found to have similar reactivity towards **2**. Although, the reaction was slightly slower (5 h at 25 °C), it resulted in high yield formation of product **5**:

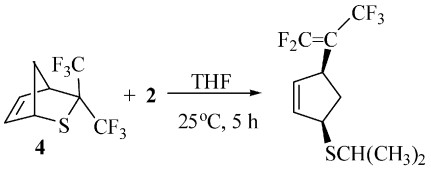

(2)

5, 77%

On the other hand, the reactivity of adduct **6** towards **2** is significantly lower, resulting in longer reaction time and lower conversion (Eq. (3)):

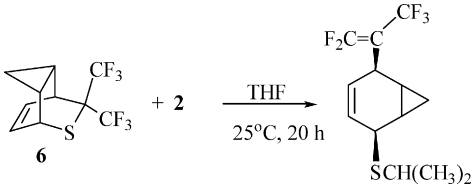

(3)

7, calc. yield 70%
at 76% conversion

Due to a small difference in boiling points of the starting material and the product pure **7** was not isolated, but was characterized by NMR spectroscopy in the mixture (see Section 3).

Among studied bicyclic adducts of HFTA cycloadduct **8** had the lowest reactivity towards Grignard reagents. No product was detected by NMR in the reaction of C_2H_5MgBr in ether (25 °C, 3 days) and slow formation of **9** was observed in reaction with **2** in THF solvent (Eq. (4)):

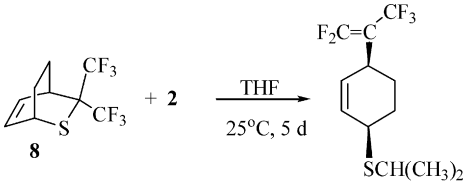

(4)

9, calc. yield 50% at
55% conversion

Monocyclic adduct **10** has the lowest reactivity towards **2**. Very slow reaction (10 days, 25 °C) led to compound **11** (Eq. (5)) in low yield. It should be pointed out that this process also had the lowest selectivity, due to formation of a noticeable amount (>10%) of byproducts derived from further reaction of **11** and **2**:

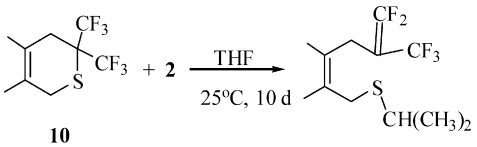

(5)

11, calc. yield 33%
at 43 % conversion

We believe, that the mechanism of reaction compounds **4**, **6**, **8**, **10** with i-C_3H_7MgCl is similar to the one suggested for **1** [6]. Exemplified by the reaction of **4** (Scheme 1), it includes initial nucleophilic attack of **2** on the sulfur atom, followed by a ring opening step producing carboanion **12**, which further undergoes F^- elimination to form final product.

It should be pointed out, that at this point an alternative mechanism based on single electron transfer can not be ruled out for this process too.

The ring opening reactions of **1**, **4**, **6**, **8** are stereoselective, producing only one isomer in each case. Based on proposed mechanism of the reaction and NMR spectroscopy data, it is believed to be the *cis*-isomer.

The observed order of reactivity towards i-C_3H_7MgCl (**1** > **4** > **6** > **8** > **10**) correlates well with decreasing of the thermodynamic driving force for the cycloadducts **1**, **4**, **6**, **8**, **10**. Figs. 1 and 2 illustrate calculated reaction entropic and Gibbs energetic driving forces for processes presented by Eqs. (1), (2), (4) and (5). As Fig. 1 indicates there is essentially no entropic driving force for reactions of **8**, **10** (Eqs. (4) and (5), respectively).

On the other hand, there is significant entropic gain in reactions of compounds **1** and **4** (Eqs. (1) and (2)) due to increased number and frequency of vibrational modes in products. Each reaction is highly exergonic as illustrated in Fig. 2, and the extent of reaction observed correlates very closely with the Gibbs energy of reaction. The relative differences in free energy release are dwarfed by the strong contribution converting the organometallic magnesium to MgClF salt. Ignoring the large internal energy reaction

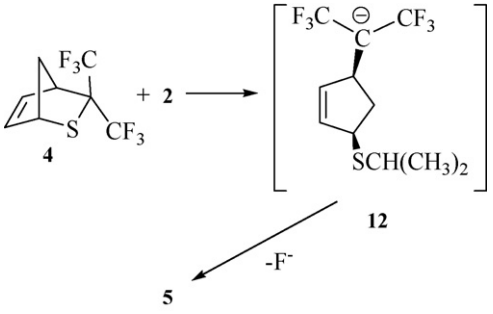

Scheme 1.

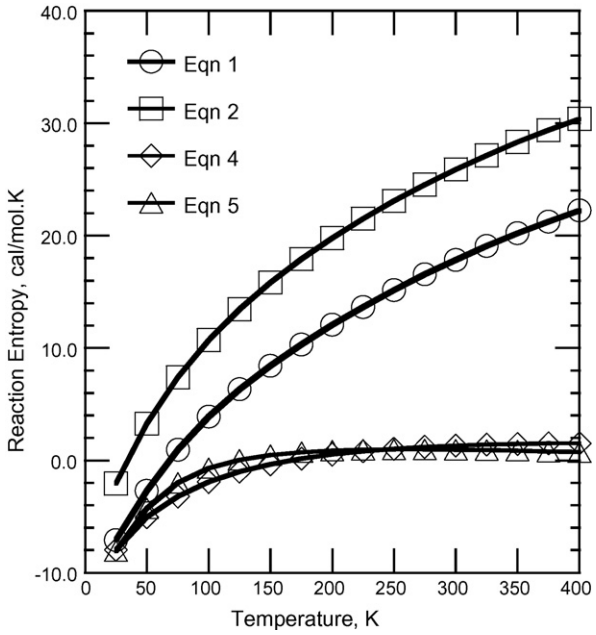

Fig. 1. Entropy of reaction calculated for reaction of compounds **1**, **4**, **8**, **10** with *i*-C_3H_7MgCl (Eqs. (1), (2), (4) and (5), respectively).

difference from this contribution and computing the remaining Gibbs reaction energy from temperature-dependent contributions including the zero-point vibrational energy corrections, we find reactions represented by Eqs. (1) and (2) are far most strongly favored and reactions of **8** and **10** (Eqs. (4) and (5)) are very minimal exergonic. There is much higher ring strain release in ring opening reactions of **1** and **4** (Eqs. (1) and (2)). The results of calculations correlate well with the experimentally observed order of reactivity. Ulterior calculations of reaction activation barrier would indicate kinetic limitations. Given that each of these reactions are predicted to be exergonic, we suspect that reactions of **8** and **10** are kinetically limited under the experimental conditions studied. Comparison of either the Mulliken population charge or the Fukui functions at the reactant sulfur does not correlate to the observed reactivity in this series of structures.

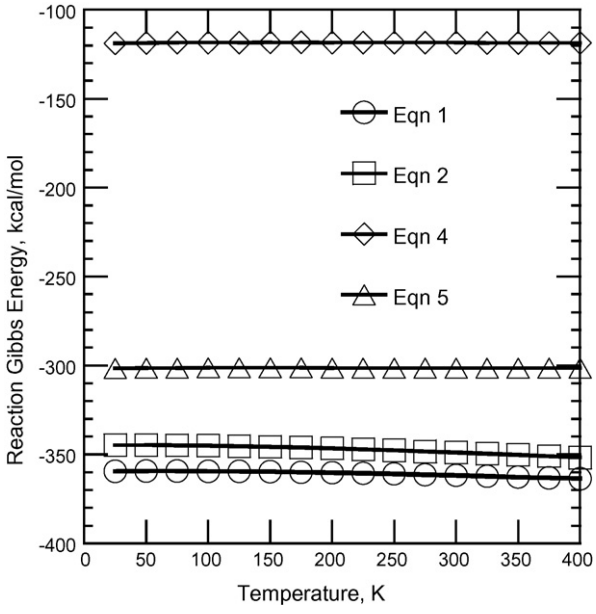

Fig. 2. Gibbs energy of reaction calculated for reaction of compounds **1**, **4**, **8**, **10** with *i*-C_3H_7MgCl (Eqs. (1), (2), (4) and (5), respectively).

2.2. Oxidation reactions

Despite of substantial positive charge on the sulfur atom, cycloadducts **1**, **4**, **6**, **8**, **10** still are able to undergo oxidation. For example, the compound **1** was converted into sulfoxide **13** using recently developed method [7]—oxidation by 30% hydrogen peroxide in hexafluoro-*iso*-propanol solvent:

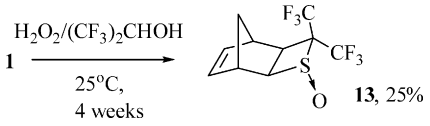

(6)

Rather slow at ambient temperature oxidation had ~85% selectivity towards **13**, due to the formation of ''over-oxidized'' products. Pure sulfoxide was isolated by column chromatography (see Section 3 and Table 3). The formation of **13** was also observed in reaction of **1** with the solution of hydrogen peroxide/urea complex in hexafluoro-*iso*-propanol (NMR), but it was significantly slower and this method did not offer any advantage over the process utilizing 30% H_2O_2.

Compound **13** forms as single isomer and the *endo*-orientation of oxygen was confirmed by single crystal X-ray diffraction (Fig. 3), indicating that the attack of oxidizer on sulfur proceeds selectively from the less hindered *endo*-face of **1**.

Similar stereoselectivity was previously observed in the oxidation of *exo*-3-aza-4-perfluoroalkyltricyclo[4.2.1.$0^{2,5}$]non-3,7-dienes by *m*-chloroperoxybenzoic acid (MCPBA) leading

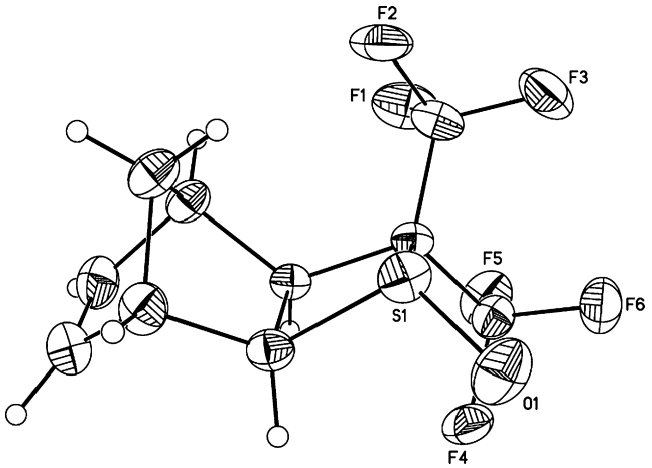

Fig. 3. ORTEP drawing of **13** with thermal ellipsoids drawn to the 50% probability level.

to the products having an *endo*-orientation of the oxygen of the oxaziridine ring [8].

The reaction of **1** with MCPBA led to complete oxidation with the formation of epoxide-sulfone **14**:

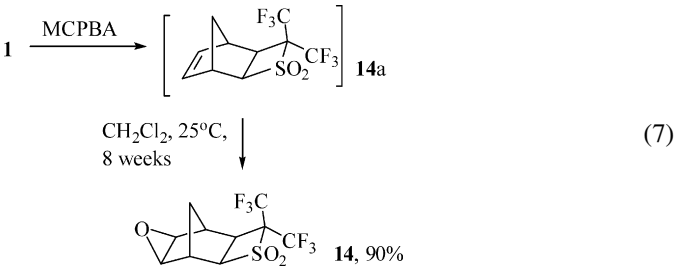

(7)

The first step of oxidation is exothermic and **1** should be added to the solution of MCPA at low temperature (see Section 3). According to NMR this step is not selective and leads to a mixture of the corresponding unsaturated sulfoxide and sulfone **14a**, along with some epoxide **14**. The last step, involving oxidation of the double bond is significantly slower and takes several weeks at ambient temperature.

It should be pointed out that, the oxidation of structurally similar cycloadducts of bis(trifluoromethyl)thioketene and quadricyclanes by MCPBA, was reported to proceed without oxidation of the double bond of norbornene fragment [9], leading to unsaturated sulfone, structurally similar to **14a**.

Compound **14** forms as a single isomer with *exo*-orientation of epoxide ring (Fig. 4). which is consistent with the stereochemistry of oxidation *exo*-3-aza-4-perfluoroalkyl-tricyclo[4.2.1.0^{2,5}]non-3,7-dienes by MCPBA leading to the corresponding products also having *exo*-orientation of epoxy ring [8].

Rather slow reaction of compound **10** and MCPBA did not stop at the stage of compound **15a** (Eq. (8)), resulting in the formation of the epoxy sulfone **15** [10]. The structure of **15** was confirmed by single crystal X-ray diffraction:

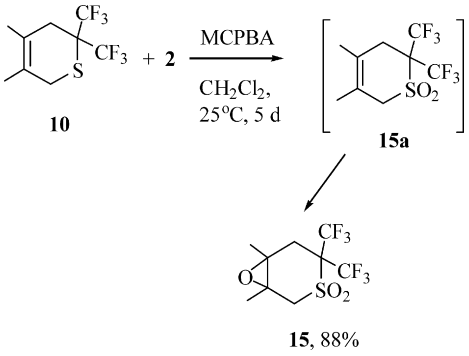

(8)

It is interesting, that the reaction of cycloadducts **4**, **6** or **8** with excess of MCPBA resulted in selective oxidation of sulfur only, leading to unsaturated sulfones **16–18** (Eq. (9)):

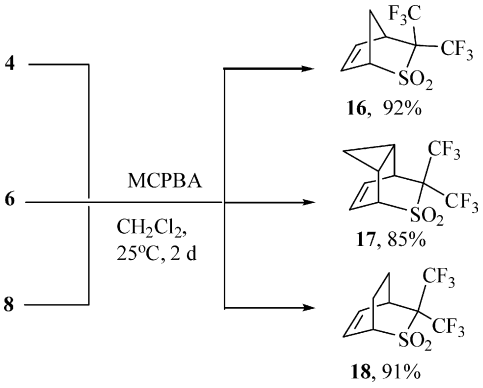

(9)

Despite the fact that the reaction of **4**, **6** or **8** with MCPBA is relatively slow (Table 3), it is surprisingly selective, leading to sulfones **16–18** in high yield. The formation of products of further oxidation of C=C was observed when isolated **16** and **18** were treated by excess of MCPBA for longer period of time (25 °C, 5 weeks, CH_2Cl_2) at low conversion of **16** (25%) and **18** (~3%). The products of oxidation were characterized further due to relatively low concentration of in the mixture.

The formation of sulfones **16–18** is consistent with result on oxidation of the cycloadduct of bis(trifluoromethyl)thioketene and cyclopentadiene by MCPBA reported to proceed with formation of the corresponding unsaturated sulfone [11].

We believe that the lower reactivity of C=C in **4**, **6** and **8** *versus* **1** is the result of higher electron deficiency the double bond in sulfones **16–18**, due to the strong electron withdrawing effect of $-C(CF_3)_2-SO_2$ fragment. Indeed, in sulfone **14a** (Eq. (7)), the double bond undergoes the oxidation and has higher reactivity, because, the $-C(CF_3)_2-SO_2$ fragment is located further away from C=C compared to compounds **4**, **6**, **8**. This conclusion is also in a good agreement with of oxidation compound **19** by excess of MCPBA, leading to selective formation of epoxide-sulfone **20**, in which selective oxidation of remote double bond was observed (Eq. (10)) and neither isomeric **20a** or bis-epoxide **20b** were detected in the crude

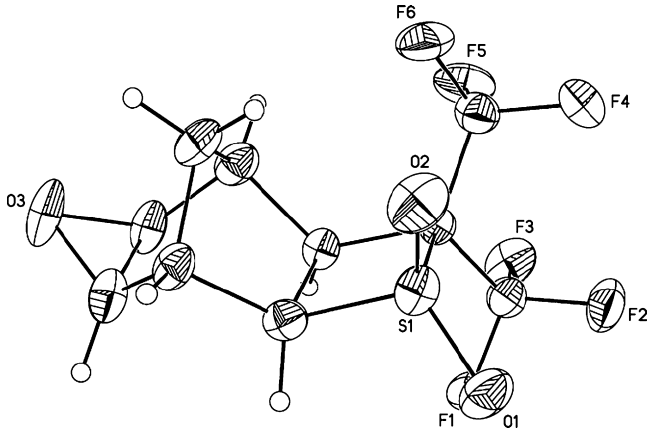

Fig. 4. ORTEP drawing of **14** with thermal ellipsoids drawn to the 50% probability level.

product (NMR):

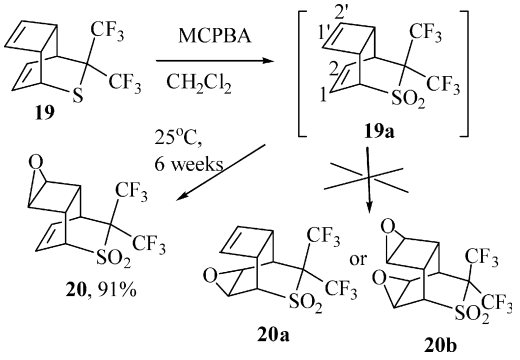

(10)

This reaction is regio- and stereo-selective, leading to the exclusive formation of single isomer **20** with an *exo*-orientation of the epoxide ring (NMR, single crystal X-ray diffraction, Fig. 5).

To rationalize the observed results of reactions compounds **1**, **4**, **6**, **8**, **10**, **19** with MCPBA a DFT study was performed. Oxidation reactions thermodynamics for processes presented by Eqs. (7)–(10) (compounds **14a**, **15a**, **16**, **17**, **18**, **19a**, **20**) are illustrated by Fig. 6.

All reactions are entropically hindered. Reaction entropies decline with increasing temperature to values between −2.5 and −4 cal/mol K, except for **15a** (which remains between zero and −1 cal/mol K. All reactions are exergonic, but to different extents between −32 and −48 kcal/mol. The range is small relative to the expected accuracy of the level of theory, typically ±10 kcal/mol. The double bond in compounds **16**, **17**, **18** was not observed to oxidize at ambient temperature however, the thermodynamic driving force is just as significant in these cases as in oxidations of materials **14a**, **15a**, **19a**. Oxidation of **19a** to **20** (Eq. (10)) is exergonic by at least 44 kcal/mol, however, the driving force for epoxidation of the double bond closest to the sulfone group to form **20a** is significantly lower at *ca*. −34 kcal/mol for both *endo*- or *exo*-epoxides; on the other hand, the driving force for oxidation on the remote C=C in the *exo*-configuration is significantly more favored at *ca*. −44 kcal/mol

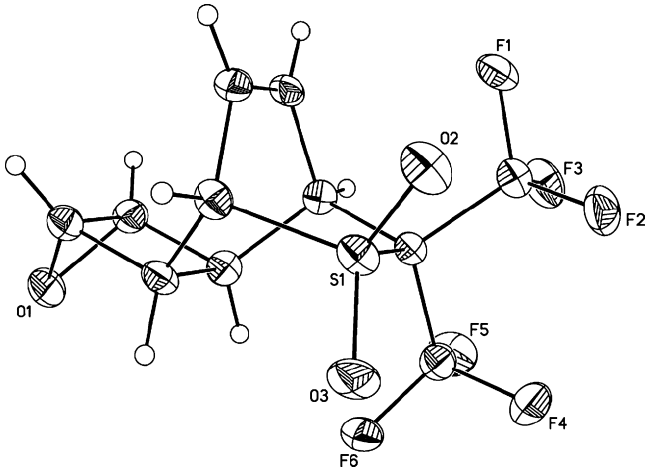

Fig. 5. ORTEP drawing of **20** with thermal ellipsoids drawn to the 50% probability level.

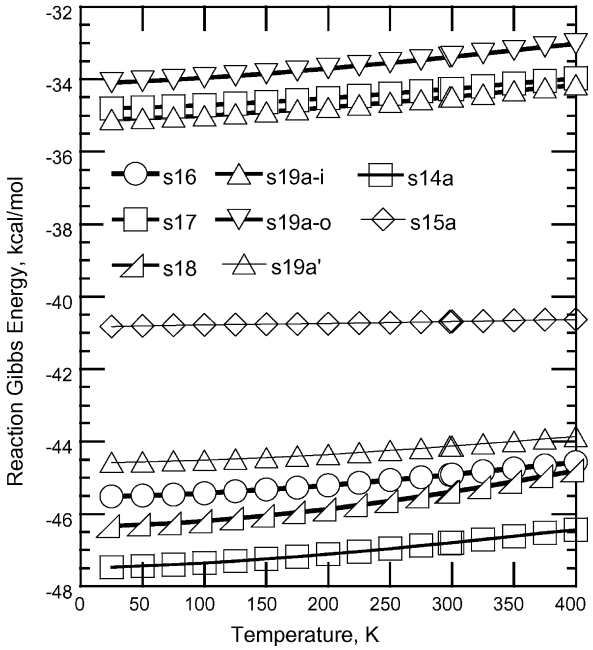

Fig. 6. Gibbs energy calculated for the epoxidation of **14a**, **15a**, **16**, **17**, **18**, **19a** by MCPBA. For reaction with structure **19a** there are three cases reported. The curve labeled s19a′ denotes the epoxidation reaction occurring on the olefin closest to the sulfone having the epoxide product **20**. The curves labeled s19a-i and s19a-o denote the reactions occurring on the olefin remote from the sulfone inside and outside of the bridges, respectively.

and this is the only material observed under the selected experimental conditions. The analysis of Mulliken population charges at the olefinic carbons in **14a**, **15a**, **16**, **17**, **18**, **19a**, **20** does not provide an easily discernible correlation to observed reactivity.

Frontier orbital analysis using Fukui functions correlates well to the observed reactivity towards epoxidation of olefinic functionality in the compounds studied. The double bonds in structures **16**, **17**, **18** (as well as the double bond closest to the SO_2 in structure **19a**) failed to oxidize under the experimental conditions even with excess of MCPBA present. The double bonds in structures **14a**, **15a** and the double bond furthest from the SO_2 in structure **19a** were reactive to epoxidation. For all these structures we compare the Fukui functions at the olefinic carbons (Table 1). In all cases in which we observed unreactive olefins the computed values of the nucleophilic reactivity indicator function, f^+ (see Section 3 for definition of f^+ and f^-), exceed the values of the electrophilic reactivity indicator function, f^-, at both unsaturated carbons. In contrast consider the reactive olefin groups in structures **14a** and **15a**. Here we observe the computed values of the electrophilic reactivity indicator function, f^-, exceed the values of the nucleophilic reactivity indicator function, f^+ at both unsaturated carbons. The reactive carbons 1′ and 2′ of structure **19a** (see Eq. (10)) are different from others studied. At carbon 1′ the nucleophilic reactivity indicator is about equal to the electrophilic reactivity indicator, while at carbon 2′ the nucleophilic reactivity indicator is greater than the electrophilic indicator. Although epoxidation is predicted to be less favorable at carbon 2′, the reactivity at carbon 1′ is apparently sufficient to proceed as

Table 1
Fukui function values at olefinic carbons for each structure and olefin reactivity to epoxidation

Structure	Carbon Label [a]	f^+	f^-	
16	1	0.135	0.093	unreactive
	2	0.162	0.108	
17	1	0.128	0.060	
	2	0.150	0.073	
18	1	0.130	0.097	
	2	0.152	0.107	
19a	1	0.089	0.081	
	2	0.109	0.088	
	1'	0.046	0.041	reactive
	2'	0.041	0.027	
14a	1	0.084	0.133	
	2	0.095	0.136	
15a	1	0.085	0.104	
	2	0.110	0.108	

[a]Carbons labeled 1 and 2 are separated from the sulfone group by one and two structural carbons, respectively. In the case of structure **19** there are two double bonds, so carbons labeled 1′ and 2′ are separated from the sulfone group by three and four structural carbons, respectively.

observed. In summary frontier orbital analysis correlates well with the electrophilic mechanism of Prilezhaev oxidation process, expected for reaction of MCPBA with electron rich double bonds. The double bonds in reactive olefins have higher electron density and the electrophilic reactivity indicator function, f^-, reflects higher susceptibility of these olefins towards oxidation. The less reactive double bond have higher values of f^+ indicating that they are more electron deficient as they would be less susceptible to electrophilic attack.

3. Experimental

^1H and ^{19}F NMR spectra were recorded on Bruker DRX-500 (499.87 MHz) and Bruker DRX-400 (376.8485 MHz) instruments respectively, using TMS and $CFCl_3$ as an internal standards and $CDCl_3$ as a lock solvent. IR spectra were recorded on a Perkin-Elmer 1600 FT spectrometer (KCl plates for liquids or KBr for solid materials). Moisture sensitive materials were handled in a glove box. The purity of isolated materials was established using NMR and GC and reported in this section. GC and GC/MS analysis were carried out on a HP-6890 instrument, using HP FFAP capillary column and either TCD (GC) or mass selective detector (GS/MS), respectively.

Compounds **1**, **4**, **6**, **8**, **10**, **19** were prepared according to literature procedure [4]. MCPBA (60–75%, Aldrich) was concentrated by washing with buffer pH 7.5 and drying under vacuum. According NMR the purity of washed material was >90%. *i*-C_3H_7-MgCl (2 M in THF) was purchased from Aldrich Co. Compounds **15** [10] and **16** [12] were identified by comparison of their melting points and NMR data with reported values. Due to the high ratio of sulfur to fluorine, elemental analysis was not attempted for the new materials. Structures of compounds **13**, **14**, **15**, **17** and **20** were established by single crystal X-ray diffraction and crystallographic data (excluding structure factors) were deposited with the Cambridge Crystallographic Data Centre as CCDC 639430–639434, respectively. Copies of the data can be obtained, free of charge, on application to CCDC, 12 Union Road, Cambridge CB2 1EZ, UK (fax: +44 1223 336033 or e-mail: deposit@ccdc.cam.ac.uk).

3.1. Computational methods

All calculations were performed using the density functional theory electronic structure program DMol[3] [13,14] with graphical displays generated with Materials Studio [15]. The Perdew–Wang (PW91) generalized gradient approximation [16] was used for the exchange and correlation potentials with restricted spin polarization and fine DNP numerical basis sets with 4 Å cut-off. Atomic cores are described with the all-electron treatment. SCF iterations were considered converged with 10^{-6} Ha tolerance and no smearing was used in the orbital occupancy. Molecular geometries were refined via energy optimizations in which convergence tolerance criteria included energy changes less than 10^{-5} Ha, maximum forces less than 0.002 Ha/Å and maximum displacements less than 0.005 Å. Thermodynamic properties such as entropy, enthalpy and Gibbs energy are computed at finite temperatures after fine geometric optimization and vibrational analysis or Hessian evaluation. Vibrational, rotational and translational contributions to the molecular partition function are computed according to standard statistical mechanics in the ideal gas approximation [17]. Fukui functions [18] are used to assess reactivity from a frontier orbital analysis. The function f^+ measures the change in the local electron density when the molecule gains electrons and, hence, corresponds to reactivity with respect to nucleophilic attack. Conversely, the function f^- measures the change in the local electron density when the molecule loses electrons, and hence, indicates the reactivity with respect to electrophilic attack. For the ensuing discussion these functions are calculated from differences in atom-centered charges. These charges are calculated from Mulliken population analysis before and after 0.1 electrons are removed (or added) for f^- (or f^+), respectively. A larger difference between the molecule's neutral and partial ion states in these atom-centered charges indicates a higher kinetic reactivity.

3.1.1. Reaction of *1*, *4*, *6*, *8*, *10* with *i*-C_3H_7MgCl (*2*), typical procedure

About 27–30 mL of 2 M solution of **2** in THF was slowly added at 0 °C to the agitated solution of sulfur-containing substrate (0.05 mol in 100 mL of dry THF) in three-neck round bottom glass flask equipped with thermocouple, additional funnel and reflux condenser. The reaction mixture was warmed up to ambient temperature and kept agitated for period specified in Table 2. It was diluted with 300 mL of 10% hydrochloric acid, extracted by CH_2Cl_2 (100 mL × 3), combined organic layer was dried over $MgSO_4$, solvent was removed under vacuum and residue was distilled under reduced pressure. The ratios of reagents and reaction conditions are given in Table 2.

Table 2
Reaction of **4**, **6**, **8** and **10** with *i*-C_3H_7MgCl

Entry	Substrate	Time	Temperature (°C)	Conversion (%)	Product (yield %)
1	**4**	5 h	0–25	100	**5** (77)
2	**6**	20 h	0–25	76	**7** (70)[a]
3	**8**	5 days	0–25	55	**9** (50)[a]
4	**10**	10 days	0–25	60	**11** (33)[a]

[a] Calculated yield (NMR).

*3.1.1.1. Isopropyl[4-(perfluoroprop-1-en-2-yl)cyclopent-2-enyl]sulfane (**5**).* b.p. 65–66/0.1 mmHg, purity >99%. ^{1}H NMR ($CDCl_3$) (ppm): 1.25 (6H, dd, J = 6.7, 2.3 Hz), 1.72 (1H, dt, J = 13.5, 8.1 Hz), 2.75 (1H, d.t, J = 13.5, 8.1 Hz), 2.95 (1H, sept., J = 6.7 Hz), 3.50 (1H, tm, J = 8.5, 2.8 Hz), 3.78 (1H, br. t, $J \sim$ 8.0 Hz) 5.62 (1H m Hz), 5.74 (1H, m). ^{19}F (ppm): −59.66 (3F, dd, J = 24.1, 10.4 Hz), −73.82 (1F, qdd, J = 24.1, 17.6, 2.8 Hz), −78.58 (1F, dq, J = 17.5, 10.4 Hz). ^{13}C ($CDCl_3$) (ppm): 23.17, 23.44, 34.86, 39.63 (t, J = 2.8 Hz), 40.08, 47.51, 89.59 (qdd, J = 30.0, 21.3, 6.8 Hz), 123.10 (qm, J = 273.2 Hz), 129.70, 134.32, 158.93 (tm, J_t = 300 Hz). IR (liq., KCl, major): 2964, 1741, 1453, 1374, 1347, 1313, 1282, 1126, 1010, 787, 743 cm^{-1}. GC/MS (EI, *m/z*): 272, 274 (M^+, $C_{11}H_{13}F_5S^+$).

*3.1.1.2. Isopropyl[(2S,5R)-5-(perfluoroprop-1-en-2-yl)bicyclo[4.1.0]hept-3-en-2-yl]sulfane (**7**).* Distillation under vacuum gave two fractions with b.p. 51–56/0.14 mmHg (**6** and **7**, ratio 1:1,) and b.p. 56–57/0.14 mmHg (**6**, 14%, **7**, 86%). ^{1}H NMR ($CDCl_3$) (ppm): 0.33 (1H, q, J = 5.2 Hz), 0.86 (1H, dq, J = 8.9, 4.6 Hz), 1.20 (1H, q, J = 6.4 Hz), 1.39 (6H, dd, J = 6.7, 1.5 Hz), 1.48 (1H, q, J = 6.4 Hz), 3.15 (1H, sept., J = 6.7 Hz), 3.40 (1H, m), 3.62 (1H, t, 4.2 Hz) 5.43 (1H, ddt, J = 10.4, 4.9, 1.8 Hz), 5.78 (1H, ddt, J = 10.4, 5.2, 2.1 Hz). ^{19}F (ppm): −59.90 (3F, dd, J = 23.5, 10.3 Hz), −73.63 (1F, qdd, J = 23.5, 13.8, 3.4 Hz), −75.42 (1F, dq, J = 13.8, 10.3 Hz). IR (liq., KCl, major): 300, 1738, 1447, 1363, 1307, 1250, 1187, 1134, 1030, 847, 787 cm^{-1}. MS (EI, *m/z*): 298 (M^+, $C_{13}H_{15}F_5S^+$), 223 [$(M - C_3H_7)^+$, $C_{10}H_8F_5^+$, 100%].

*3.1.1.3. Isopropyl[-4-(perfluoroprop-1-en-2-yl)cyclohex-2-enyl]sulfane (**9**, 1:1 mixture of **8** and **9**).* ^{1}H NMR ($CDCl_3$) (ppm): 1.30 (6H, d, J = 6.9 Hz), 1.6–2.1 (4H), 3.15 (1H, sept., J = 6.8 Hz), 3.00 (1H, m), 3.33 (1H, m) 5.50 (1H, ddt, J = 10.3 Hz), 5.77 (1H, ddd, J = 9.7, 5.1, 3.1 Hz). ^{19}F (ppm): −60.01 (3F, dd, J = 23.5, 10.5 Hz), −74.25 (1F, qdd, J = 23.5, 17.6, 2.3 Hz), −77.66 (1F, dq, J = 17.6, 10.5 Hz). MS (EI, *m/z*): 286 (M^+, $C_{12}H_{15}F_5S^+$), 211 [$(M - C_3H_7S)^+$, $C_9H_8F_5^+$, 100%].

*3.1.1.4. (Z)-6,6-Difluoro-5-(trifluoromethyl)-2,3-dimethylhexa-2,5-dienyl)(isopropyl)sulfane (**11**, characterized in mixture with **10**).* ^{1}H NMR ($CDCl_3$) (ppm): 1.20 (6H, d, J = 6.8 Hz), 2.77 (1H, sept., J = 6.8 Hz), 2.94 (2H, s), 3.17 (2H, s). ^{19}F (ppm): −61.23 (3F, dd, J = 22.0, 10.3 Hz), −77.90 (1F, quint., J = 22.0 Hz), −82.46 (1F, m, J = 10.2 Hz). GC/MS (EI, *m/z*): 288 (M^+, $C_{12}H_{17}F_5S^+$).

*3.1.2. Preparation of sulfoxide **13***

A mixture of 20 mL of hexafluoro-*iso*-propanol, 5 mL of 30% H_2O_2 and 6 g (0.021 mol) of **1** was agitated at ambient temperature for 4 weeks. The reaction mixture was diluted with 100 mL of water, extracted by CH_2Cl_2 (50 mL × 3), combined organic layer washed with sodium 0.1 molar thiosulfate solution (100 mL × 3, KI peroxide test was negative). The reaction mixture was washed with saturated solution of $NaHCO_3$ (100 mL × 3), dried over $MgSO_4$, solvent was removed under vacuum to leave 6 g of crude **13** of 85% purity. Purification of **13** by column chromatography gave 3.5 g of material 94% purity (eluent hexane) and 1.5 g of pure **13** (eluent toluene). Calculated yield 80%, isolated yield 25%; m.p. 54–55 °C, purity >99%, ^{1}H NMR ($CDCl_3$) (ppm): 1.72 (2H, A:B pattern, J = 11.0 Hz), 2.90 (1H, d, J = 9.2 Hz), 3.28 (1H, s), 3.35 (1H, d, J = 9.2 Hz), 3.53 (1H, sept., J = 1.2 Hz), 6.17 (1H, dd, J = 5.5, 3.1 Hz), 6.42 (1H, dd, J = 5.5, 3.3 Hz). ^{19}F (ppm): −64.03 (3F, q, J = 9.8 Hz), −65.90 (3F, q, J = 9.8 Hz). ^{13}C ($CDCl_3$) (ppm): 37.99, 41.78, 44.19, 44.42 (q, J = 3.0), 62.94, 69.26 (sept., J = 27.0), 122.32 (qq, J = 284, 2.7 Hz), 122.38 (qq, J = 284, 1.9 Hz), 134.96, 140.01. IR (CH_2Cl_2): 1085 cm^{-1} (S=O). GC/MS (EI, *m/z*): 290 $(C_{10}H_8F_6OS)^+$.

3.1.3. Oxidation using MCPBA (typical procedure)

To solution of sulfur-containing substrate (0.02 mol in 60 mL of CH_2Cl_2) placed in three-neck round bottom glass flask equipped with thermocouple, additional funnel and reflux condenser was slowly added at 0 °C the solution of 10 g of MCPBA in 50 mL of CH_2Cl_2. The reaction mixture was warmed up to and agitated at ambient temperature for period of time specified in Table 3. The precipitate was filtered off and the reaction mixture was washed with sodium thiosulfate solution (0.1 molar, 100 mL × 3, KI peroxide test was negative). The reaction mixture was washed with saturated solution of $NaHCO_3$ (100 mL × 3), dried over $MgSO_4$, solvent was removed under vacuum and residue recrystallized from hexane. The ratios of reagents and reaction conditions are given in Table 3.

*3.1.4. Compound **14***

m.p. 154–155 °C, purity >99%. ^{1}H NMR ($CDCl_3$) (ppm): 1.58 (1H, d, J = 2.0 Hz), 2.40 (1H, d, J = 12.0 Hz), 2.60 (1H, d, J = 8.2 Hz), 3.04 (1H, s), 3.14 (1H, d, J = 3.4 Hz), 3.20 (1H, d, J = 3.4 Hz), 3.26 (1H, m, J = 1.2Hz), 4.67 (1H, d, J = 8.2 Hz).

Table 3
Reaction of **1**, **4**, **6**, **8**, **10** and **19** with MCPBA

Entry no.	Substrate (mol)	MCPBA (mol)[a]	Temperature (°C)	Time	Product (yield %)
1	**1** (0.02)	0.09	0–25	2 months	**14** (90)
2	**4** (0.02)	0.07	0–25	2 days	**16** (92)
3	**6** (0.02)	0.08	0–25	2 days	**17** (85)
4	**8** (0.02)	0.07	0–25	2 days	**18** (91)
5	**10** (0.021)	0.08	0–25	5 days	**15** (88)
6	**19** (0.02)	0.07	0–25	6 weeks	**20** (91)

[a] Calculated on 95% MCPBA.

^{19}F (ppm): −61.23 (3F, q, J = 10.3 Hz), −67.10 (3F, q, J = 10.3 Hz). ^{13}C ($CDCl_3$) (ppm): 21.52 (q, J = 3.9), 33.41, 39.01, 40.84, 47.96, 55.78, 86.29, 120.98 (q, J = 286 Hz), 121.83 (q, J = 286 Hz). GC/MS (EI, m/z): 257 [$(M - HSO_2)^+$, $C_{10}H_8F_6O^+$], 189 ($C_9H_8F_3O^+$, 100%).

3.1.5. Compound **17**

m.p. 133–135 °C (from hexane), purity 99% (NMR). ^{1}H NMR ($CDCl_3$) (ppm): 0.53 (1H, m), 0.70 (1H, dt, J = 8.1, 7.3 Hz), 1.55 (1H, m), 1.82 (1H, sept., J = 3.7 Hz), 3.75 (1H, dt, 4.8, 4.2 Hz), 4.12 (1H, dt, J = 4.8, 4.2 Hz), 5.98 (2H, dd, J = 3.6, 5.6 Hz). ^{19}F (ppm): −58.48 (3F, q, J = 13.6 Hz), −61.54 (3F, qd, J = 13.6, 1.3 Hz). ^{13}C ($CDCl_3$) (ppm): 18.86, 19.49 (q, J = 2.7), 35.10, 57.30, 67.97 (sept., J = 23.3), 120.52 (q, J = 287 Hz), 120.65 (q, J = 287 Hz), 123.95, 134.33. IR (KBr): 1442 cm^{-1}. GC/MS (EI, m/z): 242 [$(M - SO_2)^+$, $C_{10}H_8F_6^+$].

3.1.6. Compound **18**

m.p. 181–182 °C (from hexane), purity 98% (NMR). ^{1}H NMR ($CDCl_3$) (ppm): 1.41 (1H, q, J = 12.2 Hz), 1.88 (1H, td, J = 12.2, 4.9 Hz), 2.20 (1H, t, J = 12.3 Hz), 2.59 (1H, quint., J = 5.6 Hz), 3.36 (1H, dt, 7.0, 2.9 Hz), 3.90 (1H, t, J = 6.0 Hz), 6.31 (1H, t, J = 7.7 Hz), 6.54 (1H, m). ^{19}F (ppm): −61.61 (3F, q, J = 13.1 Hz), −62.74 (3F, qd, J = 13.1, 2.6 Hz). ^{13}C ($CDCl_3$) (ppm): 19.86, 20.90 (q, J = 2.8 Hz), 36.38, 58.55, 69.37 (sept., J = 25.4 Hz), 122.40 (q, J = 286 Hz), 122.70 (q, J = 286 Hz), 125.33, 135.74. IR (KBr): 1478, 1457 cm^{-1}. GC/MS (EI, m/z): 230 [$(M - SO_2)^+$, $C_9H_8F_6^+$].

3.1.7. Compound **20**

m.p. 174–175 °C (from hexane), purity 99% (NMR). ^{1}H NMR ($CDCl_3$) (ppm): 3.00 (H, m, J = 2.2 Hz), 3.29 (1H, q, J = 3.7 Hz), 3.72 (3H, m), 4.16 (1H, d, quint., J = 5.8, 2.8 Hz) 6.51 (1H, m, Hz). ^{19}F (ppm): −59.65 (3F, q, J = 13.2 Hz), −62.08 (3F, dq, J = 13.2, 2.3 Hz). ^{13}C ($CDCl_3$) (ppm): 36.71, 39.94 (q, J = 3.9 Hz), 41.36, 54.04, 55.96, 58.57, 67.38 (sept., J = 25.2 Hz), 121.57 (q, J = 288.0 Hz), 121.70 (q, J = 288.0 Hz) 125.51, 131.54. IR (KBr, pellet, major): 3089, 2986, 1349, 1247, 1197, 1132, 944, 816, 708 cm^{-1}. GC/MS (EI, m/z): 269 [$(M - HSO_2)^+$, $C_{11}H_7F_6O^+$], 201 ($C_{10}H_8F_3O^+$, 100%).

References

[1] W.J. Middleton, J. Org. Chem. (1965) 1390–1394.
[2] T. Kitazume, N. Ishikawa, Chem. Lett. (3) (1973) 267–268.
[3] T. Kitazume, T. Otaka, R. Takei, N. Ishikawa, Bull. Chem. Soc. Jpn. 49 (1976) 2491–2494.
[4] V.A. Petrov, W. Marshal, J. Fluorine Chem. 128 (2007) 729–735.
[5] V.A. Petrov, C.G. Krespan, W. Marshall, J. Fluorine Chem. 126 (2005) 1332–1341.
[6] V.A. Petrov, Mendeleev Commun. (2006) 155–157.
[7] J.-P. Begue, D. Bonnet-Delpon, B. Crousse, Handbook of Fluorous Chemistry, 2004, pp. 341–350.
[8] V.A. Petrov, in: Current Fluoroorganic Chemistry. New Synthetic Directions, Technologies, Materials and Biological Applications, ACS Simposium Series, vol. 49, 2006, pp. 113–140.
[9] M.S. Raasch (to DuPont), US Patent 3406184 (1968).
[10] M. Schwab, W. Sundermeyer, Chem. Ber. 119 (1986) 2458–2465.
[11] M.S. Raasch, J. Org. Chem. 40 (1975) 161–172.
[12] B.E. Smart, W.J. Middleton, J. Am. Chem. Soc. 109 (1987) 4982–4992.
[13] B. Delley, J. Chem. Phys. 92 (1990) 508.
[14] B. Delley, J. Chem. Phys. 113 (2000) 7756.
[15] Accelrys Software Inc., Accelrys, MS Modeling, Release 3.1, San Diego, 2005.
[16] J.P. Perdew, Y. Wang, Phys. Rev. B 45 (1992) 13244.
[17] T. Hirano, MOPAC Manual, 7th ed., 1993.
[18] R.G. Parr, W. Yang, Density-Functional Theory of Atoms and Molecules, 1989.